

The Teddy-Tool v1.1: temporal disaggregation of daily climate model data for climate impact analysis

hat gelöscht: 0

Florian Zabel¹, Benjamin Poschlod²

¹Ludwig-Maximilians-Universität München (LMU), Department of Geography, Luisenstr. 37, 80333 Munich, Germany

²Research Unit Sustainability and Climate Risks, Center for Earth System Research and Sustainability, Universität Hamburg, Grindelberg 5, 20144 Hamburg, Germany

Correspondence to: Florian Zabel (f.zabel@lmu.de)

Abstract

Climate models provide required input data for global or regional climate impact analysis in temporally aggregated form, often in daily resolution to save space on data servers. Today, many impact models work with daily data, however, sub-daily climate information is getting increasingly important for more and more models from different sectors, such as the agricultural, the water, and the energy sector. Therefore, the open source Teddy-Tool (temporal disaggregation of daily climate model data) has been developed to disaggregate (temporally downscale) daily climate data to sub-daily hourly values. Here, we describe and validate the temporal disaggregation, which is based on the choice of daily climate analogues. In this study, we apply the Teddy-Tool to disaggregate bias-corrected climate model data from the Coupled Model Intercomparison Project Phase 6 (CMIP6). We choose to disaggregate temperature, precipitation, humidity, longwave radiation, shortwave radiation, surface pressure, and wind speed. As a reference, globally available bias-corrected hourly reanalysis WFDE5 data from 1980-2019 are used to take specific local and seasonal features of the empirical diurnal profiles into account. For a given location and day within the climate model data, the Teddy-Tool screens the reference data set to find the most similar meteorological day based on rank statistics. The diurnal profile of the reference data is then applied on the climate model. The physical dependency between variables is preserved, since the diurnal profile of all variables is taken from the same, most similar meteorological day of the historical reanalysis dataset. Mass and energy are strictly preserved by the Teddy-Tool to exactly reproduce the daily values from the climate models.

hat gelöscht: on a daily basis

hat nach unten verschoben [5]: Thereby, mass and energy are strictly preserved by the Teddy-Tool to exactly reproduce the daily values from the climate models.

hat gelöscht: for temperature, precipitation, humidity, longwave radiation, shortwave radiation, surface pressure and wind speed.

hat gelöscht: document

hat formatiert: Schriftfarbe: Automatisch

hat gelöscht:

hat gelöscht: Therefore

hat gelöscht: course

hat gelöscht: empirically

hat verschoben (Einfügung) [5]

hat gelöscht: Thereby,

hat gelöscht: mMass and energy are strictly preserved by the Teddy-Tool to exactly reproduce the daily values from the climate models. ...

hat gelöscht:

hat gelöscht: ,

hat gelöscht: and extreme value

hat gelöscht: However,

hat gelöscht: w

hat gelöscht: also

hat gelöscht: Consequently

hat formatiert: Schriftart: Fett

Formatiert: Listenabsatz, Nummerierte Liste + Ebene: 1 + Nummerierungsformatvorlage: 1, 2, 3, ... + Beginnen bei: 1 + Ausrichtung: Links + Ausgerichtet an: 0,63 cm + Einzug bei: 1,27 cm

For evaluation, we aggregate the hourly WFDE5 data to daily values and apply the Teddy-Tool for disaggregation. Thereby, we compare the original hourly data with the data disaggregated by Teddy. We perform a sensitivity analysis of different time window sizes used for finding the most similar meteorological day in the past. In addition, we perform a cross-validation and autocorrelation analysis for 30 globally distributed samples around the world, representing different climate zones. The validation shows that Teddy is able to reproduce historical diurnal courses with high correlations >0.9 for all variables, except for wind speed (>0.75) and precipitation (>0.5). We discuss limitations of the method regarding the reproduction of precipitation extremes, inter-day connectivity, and disaggregation of end-of-century projections with strong warming. Depending on the use case, sub-daily data provided by the Teddy-Tool could make climate impact assessments more robust and reliable.

1. Introduction

65 Sub-daily climate data is becoming increasingly important in climate impact analysis. This type of data,
66 which captures variations in temperature, precipitation, and other weather variables at intervals of
67 less than a day, can provide a more detailed representation of local and regional climate conditions
68 and temporal variations. This information can be crucial for evaluating the impacts of climate change
69 on various sectors, such as agriculture, water resources, energy production, and human health (Golub
70 et al., 2022; Trinanes and Martinez-Urtaza, 2021; Colón-González et al., 2021; Tittensor et al., 2021;
71 Byers et al., 2018; Jägermeyr et al., 2021; Poschlod and Ludwig, 2021; Degife et al., 2021). A better
72 representation of the diurnal course of temperature, extreme precipitation events, and other weather
73 variables are also important for adaptation assessments which depend on behavior or processes with
74 high temporal dynamics, such as the energy demand, labor activity, the heat stress of crops or flood
75 events (Minoli et al., 2022; Zabel et al., 2021; Reed et al., 2022; Orlov et al., 2021; Franke et al., 2022;
76 [Poschlod 2022](#)). Research has shown that using sub-daily climate data can result in more robust and
77 reliable impact assessments compared to using daily data (Orlov et al. 2023).

78 Today, most climate model data are available for download at daily resolution because of the high
79 storage requirements for sub-daily climate data ([Juckes et al., 2020](#)). However, the demand for sub-
80 daily data is increasing ~~with future developments of data management expected to handle this~~
81 ~~demand with decreasing~~ costs for storage and computing resources ([Lüttgau & Kunkel, 2018](#)). Different
82 methods exist to disaggregate available daily climate data to sub-daily, most often hourly values. These
83 can be roughly divided into statistical methods, weather generators, and mechanistic approaches,
84 although mixed forms also exist (Förster et al., 2016).

85 Mechanistic methods use regional climate models to dynamically downscale atmospheric conditions
86 in time and space, usually for a limited area (Vormoor and Skaugen, 2013; Liu et al., 2011; Kunstmann
87 and Stadler, 2005). Weather generators generate synthetic sequences of hourly weather variables by
88 using random number generators that match statistics (Ailliot et al., 2015; Mezghani and Hingray,
89 2009). Various statistical methods exist for temporal disaggregation of daily climate data, ranging from
90 simple interpolations or deterministic approaches to non-parametric approaches and methods that
91 derive statistical relationships from historical data [or look for climate analogues](#) ([Bennett et al., 2020](#);
92 [Breinl and Di Baldassarre, 2019](#); [Chen, 2016](#); [Debele et al., 2007](#); [Förster et al., 2016](#); [Görner et al.,](#)
93 [2021](#); [Liston and Elder, 2006](#); [Park and Chung, 2020](#); [Verfaillie et al., 2017](#); [Poschlod et al., 2018](#); [Zhao](#)
94 [et al., 2021](#)). Each of these methods has its own advantages and limitations, and the choice of method
95 depends on factors such as the specific needs of the impact assessment, the quality of the available
96 data, and computational resources.

97 Here, we introduce the Teddy-Tool (**temporal disaggregation of daily climate model data**), which uses
98 statistical methods for temporal disaggregation of daily climate model data. Existing statistical
99 approaches are often only valid for a specific location and cannot be applied globally. In addition,
100 available disaggregation tools often focus on only one variable ([e.g. Pui et al., 2012](#)) and therefore do
101 not consider physical interdependencies between different variables, such as precipitation, humidity,
102 temperature, and radiation. Teddy has been specifically developed as a globally applicable tool for
103 climate impact studies. For this purpose, Teddy strictly preserves mass and energy of daily climate
104 model data for each variable throughout the disaggregation procedure. Teddy additionally aims at
105 taking regional and seasonal climate characteristics into account and considers the physical
106 consistency between variables.

hat gelöscht: due to

hat gelöscht: lower

109 Teddy represents an easy-to-use tool that can be applied for climate impact assessments in different
 110 sectors that allows a physically consistent temporal disaggregation of daily climate model data. The
 111 Teddy-Tool has been written in Matlab and is available open source via Zenodo ([see code availability](#)).

112 2. Data and data requirements

113 In principle, the Teddy-Tool can be used with any climate input, but has specifically been developed to
 114 be used with daily climate data for historical time periods and future scenarios from the Inter-Sectoral
 115 Impact Model Intercomparison Project (ISIMIP). ISIMIP offers a framework for consistently projecting
 116 the impacts of climate change across affected sectors and spatial scales (Warszawski et al., 2014). To
 117 guarantee cross-sectoral consistency in ISIMIP, all sectors are provided with the same climate data for
 118 historical (1850-2014) and future time periods (2015-2100) for different scenarios (SSP126, SSP370,
 119 SSP585). ISIMIP provides bias-corrected climate model data from the Coupled Model Intercomparison
 120 Project Phase 6 (CMIP6) and trend-preserving reanalysis climate data (Lange, 2019). Within ISIMIP,
 121 some modeling communities from different sectors have expressed their need for sub-daily climate
 122 data, including the agricultural and the energy sector.

123 Daily bias-corrected climate model data are provided by ISIMIP at 0.5° spatial resolution for air
 124 temperature (tas), humidity (hurs), shortwave radiation (rsds), longwave radiation (rls), air pressure
 125 (ps), wind speed (sfcwind), and precipitation (pr) (Lange, 2019). For air temperature, the daily
 126 maximum (tasmax) and minimum (tasmin) values are additionally provided. ISIMIP provides CMIP6
 127 data for the climate models GFDL-ESM4, IPSL-CM6A-LR, MPI-ESM1-2-HR, MRI-ESM2-0, and UKESM1-
 128 0-LL.

129 Teddy requires hourly climate data as a reference for temporal disaggregation. Therefore, we use the
 130 WFDE5 dataset, which has been generated using the WATCH Forcing Data (WFD) methodology applied
 131 to ERA5 reanalysis data (Cucchi et al., 2020). The bias-adjusted hourly WFDE5 data is globally available
 132 for the time period between 1979 and 2019 at 0.5° spatial resolution. It is consistent with the bias-
 133 adjustment procedure within ISIMIP (Lange, 2019) and thus provides a consistent hourly reference
 134 data for Teddy. Table 1 gives an overview of the available variables and the required datasets at their
 135 temporal resolution. The temporal resolution of the Teddy output is adjustable by the user and can be
 136 set to 1-, 2-, 3-, 4-, 6-, 8-, or 12-hourly values.

137 Table 1: Variables and units of used hourly (h) and daily (d) climate data and the Teddy output. For
 138 WFDE5, the specific variable name is provided in brackets. WFDE5 variables have instantaneous values,
 139 while SWdown, LWdown, Rainf and Snowf have average values over the next hour at each time step.

Variable	WFDE5 (h)	ISIMIP Climate Model (d)	Teddy (flexible)
Air temperature (tas)	K (Tair)	K	K
tasmin	=	K	=
tasmax	=	K	=
Humidity (hurs/huss)	kg/kg (Qair)	%	%
Shortwave radiation (rsds)	W m ⁻² (SWdown)	W m ⁻²	W m ⁻²

hat nach unten verschoben [3]: In principal, the Teddy-Tool can be used with any climate input, but has particularly been used so far with bias corrected daily CMIP6 climate data (Eyring et al., 2016) for historical time periods and future scenarios from the ISIMIP (Inter-Sectoral Impact Model Intercomparison Project), which provides bias corrected and trend-preserved climate data (Lange, 2019) and offers a framework for consistently projecting the impacts of climate change across affected sectors and spatial scales (Warszawski et al., 2014). To guarantee cross-sectoral consistency, all sectors are provided with the same climate data. Within ISIMIP, some models from different sectors have expressed their need for sub-daily climate data, including the agricultural and the energy sector.

hat gelöscht: the ...aily ISIMIP ...limate model data. The Teddy-Tool has been written in Matlab and is available open source via Zenodo (<https://doi.org/10.5281/zenodo.76>) (... [1])

hat formatiert: Schriftart: Fett

Formatiert: Listenabsatz, Nummerierte Liste + Ebene: 1 + Nummerierungsformatvorlage: 1, 2, 3, ... + Beginnen bei: 1 + Ausrichtung: Links + Ausgerichtet an: 0,63 cm + Einzug bei: 1,27 cm

hat verschoben (Einfügung) [3]

hat gelöscht: al

hat gelöscht: particularly...pecifically been used...eveloped so far ...o be used with bias corrected ...aily CMIP6 ...limate data (Eyring et al., 2016) ...or historical time periods and future scenarios from the ISIMIP (... [2])

hat gelöscht: ,

hat gelöscht: ,

hat gelöscht: which provides bias corrected and trend-preserved climate data (Lange, 2019) and

hat formatiert (... [3])

hat gelöscht: ed

hat gelöscht: To guarantee cross-sectoral consistency (... [4])

hat verschoben (Einfügung) [2]

hat gelöscht: Teddy uses an empirical approach, whic (... [5])

hat gelöscht: As a reference,

hat gelöscht: ¶

hat verschoben (Einfügung) [4]

hat gelöscht: globally available hourly bias-corrected (... [6])

Formatiert: Links

Formatierte Tabelle

hat formatiert: Schriftart: Fett, Großbuchstaben

Formatiert: Links

Formatiert: Links

Formatiert: Links

Formatiert: Links

Formatiert: Links

Longwave radiation (rlds)	W m ⁻² (LWdown)	W m ⁻²	W m ⁻²
Precipitation (pr)	kg m ⁻² s ⁻¹ (Rainf+Snowf)	kg m ⁻² s ⁻¹	mm timestep ⁻¹
Air pressure (ps)	Pa (PSurf)	Pa	hPa
Wind speed (sfcwind)	m s ⁻¹ (Wind)	m s ⁻¹	m s ⁻¹

Formatiert: Links

Formatiert: Links

Formatiert: Links

Formatiert: Links

hat gelöscht: <#>¶

hat formatiert: Schriftart: Fett

hat gelöscht: Temporal disaggregation¶

hat gelöscht: region

hat gelöscht: from the most similar meteorological day in the past ...

hat nach oben verschoben [2]: Teddy uses an empirical approach, which applies the region-specific diurnal course from the most similar day in the past to daily climate model data for a day of interest. Teddy has been developed specifically to disaggregate daily bias-corrected climate model data from the ISIMIP project at 0.5° spatial resolution for air temperature (tas), humidity (hurs), shortwave radiation (rsds), longwave radiation (rlds), air pressure (ps), windspeed (sfcwind), and precipitation (pr) (Lange, 2019). For air temperature, the daily maximum and minimum values (tasmax, tasmin) are additionally provided. ISIMIP provides data for different historical and future time periods and scenarios for the climate models GFDL-ESM4, IPSL-CM6A-LR, MPI-ESM1-2-HR, MRI-ESM2-0, and UKESM1-0-LL. As a reference, globally available hourly bias-corrected reanalysis WFDE5 data (1980-2019) are used at 0.5° spatial resolution to identify the most similar meteorological day in the past for a specific location (Cucchi et al., 2020).

hat gelöscht: The diurnal profile of the most similar meteorological day is subsequently applied to the daily climate model data for each of the variables.

hat nach oben verschoben [4]: Table 1: Variables and units of used hourly (h) and daily (d) climate data and the Teddy output. For WFDE5, the specific variable name is

hat gelöscht: Variable ... [7]

hat gelöscht: basic population

hat gelöscht: basic population

hat gelöscht: "

hat gelöscht: "

hat gelöscht: basic population

hat gelöscht: over all variables

hat gelöscht:

hat gelöscht: basic population

hat gelöscht: T

hat gelöscht: is determined

hat gelöscht: the lowest lowest cumulated ranks

hat formatiert: Englisch (USA)

hat gelöscht: '

hat formatiert: Englisch (USA)

hat gelöscht: Hence, it does not account for the large ... [8]

265

3. Methods

Teddy uses an empirical approach, which 1) selects the 'most similar meteorological day' for the daily climate model data (here: ISIMIP CMIP6 data) within the reference climate data (here: WFDE5) at the same location. 2) Teddy applies the location-specific diurnal course to each variable of the daily climate model data for a day of interest. In the following, the procedure is explained in detail, where the example case of ISIMIP climate data and WFDE5 reference data is used for further illustration:

In a first precalculation step, in order to minimize computational resources, hourly WFDE5 data are aggregated to daily values and stored as NetCDF files. The daily aggregation uses mean values for all variables and daily sums for precipitation. In addition, rainfall and snowfall fluxes must be summed up for WFDE5. Daily maximum and minimum temperature are calculated from the hourly data. Units of climate inputs are converted to match the Teddy output (see Tab. 1). For the conversion of specific humidity to relative humidity, the Buck equation is applied (Buck, 1981).

After reading the daily climate model data for the selected location (latitude/longitude) that determines a specific grid cell at 0.5° resolution, the daily mean values of all ISIMIP variables (see Tab. 1) are compared to the aggregated daily values of WFDE5 for a specific time step in order to identify the most similar meteorological day. For the comparison, a day-of-year (DOY) window can be selected by the user that allows for a selection of days around the DOY of the actual time step. By default, the DOY window size is set to 11, which means a sequence of ± 11 days around the actual DOY. As a result, 23 days are selected from each of the 40 WFDE5 reference years (1980-2019). These 920 days now serve as the statistical population for further calculations (Fig. 1). In a next step, the climate model day of interest and the statistical population of 920 WFDE5 days are classified according to their precipitation state (wet / dry). As climate models tend to produce too many days with low-intensity precipitation called 'drizzle bias' (Chen et al., 2021), days with aggregated daily precipitation values below 1 mm per day are considered as dry days (Sun et al., 2006). Depending on the precipitation state of the previous day, the day of interest and the following day, there are eight classes: dry-dry-dry, dry-dry-wet, wet-dry-dry, wet-dry-wet, dry-wet-dry, dry-wet-wet, wet-wet-dry, and wet-wet-wet. This step is included to better reproduce the inter-day connectivity of precipitation (Li et al., 2018). Only days with the same precipitation class as the climate model day of interest are selected for the further course. Next, the absolute error (AE) between daily climate model and aggregated daily WFDE5 data for each variable is calculated for the remaining statistical population and ranked in ascending order.

The ranking approach is chosen, since the absolute or relative errors of different meteorological variables cannot be compared to each other. The ranks are cumulated with equal weight over all variables for each day of the statistical population. In this context, we define 'the most similar meteorological day' as the day with the minimum sum of ranks (Fig. 1). Thus, the 'most similar meteorological day' refers to the statistically derived similarity of all available daily near-surface meteorological variables at a given location and time. The approach works under the assumption that

354 similar daily values would have a similar sub-daily profile (Li et al., 2018; Pui et al., 2012; Sharma et al.,
355 2006). Finally, the hourly values are taken from the most similar meteorological day of the WFDE5
356 reference dataset for each variable and are divided by the WFDE5 daily mean (sum for precipitation)
357 value of the selected day, in order to refer to relative diurnal profiles without absolute variations (Fig.
358 1). The hourly profile is then applied for each variable to the daily mean (sum for precipitation) value
359 from the climate model. Thus, the daily mean value (sum for precipitation) of the climate model is
360 conserved and reproduced by the disaggregated values.

361 For temperature, the resulting hourly temperature is further scaled between the provided minimum
362 and maximum. The scaling is performed in a way that the daily mean value is preserved with an
363 accuracy of four decimals. Relative humidity is limited to 100%, considering the preservation of the
364 daily mean value.

365 Large selected DOY windows increase the statistical population, but on the other sight might distort
366 climatic characteristics with a strong seasonal course such as shortwave radiation values for the actual
367 DOY. Therefore, we preprocessed hourly potential (cloud free) solar radiation for each DOY globally at
368 0.5° spatial resolution. This data is used as upper bound to limit the resulting hourly values for the
369 corresponding DOY, while the daily mean value is preserved.

370 In a final step, the hourly values are aggregated to the temporal resolution as set by the user.

hat gelöscht:

hat gelöscht:

hat gelöscht: is conserved

hat gelöscht:

hat gelöscht: again under

hat gelöscht: preserving

hat gelöscht: .

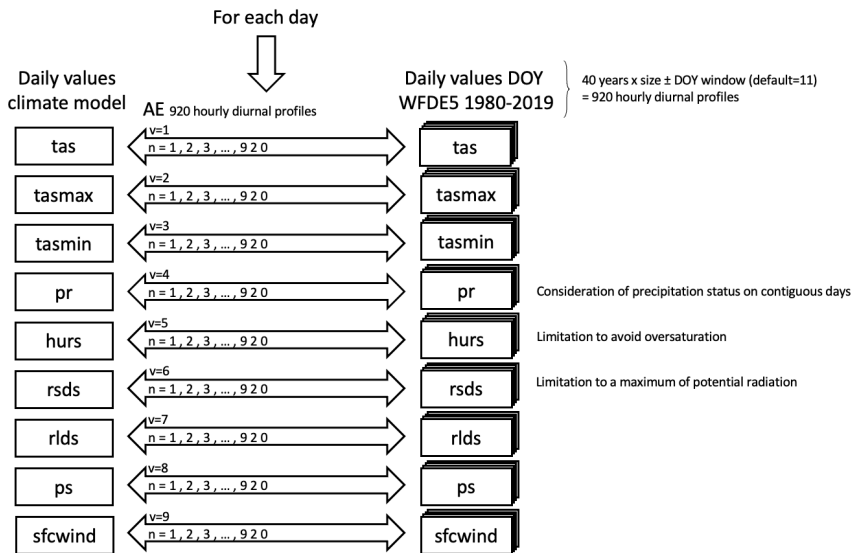
hat gelöscht: basic population

hat gelöscht:

hat gelöscht: can again be aggregated to the time step set by the user...

hat gelöscht: (possible: 1, 2, 3, 4, 6, 8, 12)

hat gelöscht:



Find most similar day

$$\text{best fit} = \min_n \left\{ \sum_{v=1}^9 (\text{rank}(AE_{v(n)})) \right\}_{n=1}^{920}$$

Select WFDE5 hourly profile for most similar day

$$\text{hourly profile} = \frac{\text{hourly values}}{\text{daily mean}} \quad (\text{daily sum for precipitation})$$

$$\text{hourly values} = \text{hourly profile} * \text{daily mean}$$

384

385 Figure 1: Procedure to identify the most similar meteorological day in the population of **WFDE5**
 386 reference data for the default DOY window of ± 11 days around the actual DOY. Daily values refer to
 387 daily sum for precipitation and daily mean values for all other variables.

388 In rare cases, precipitation cannot be distributed, due to **no** precipitation in the reference data. This
 389 can happen in dry deserts, where 40 years of WFDE5 data show no precipitation record within the
 390 range of the moving DOY window (Supplementary Fig. S1 shows a map where this is the case). To
 391 handle this exception, several options are implemented. First, the DOY window is automatically
 392 expanded to +50 days around the actual DOY in order to increase the statistical population and thus
 393 the probability to include a precipitation event. If still no precipitation event is found in the reference,
 394 a linear regression between the precipitation amount and the **precipitation** duration is performed for
 395 the specific location across the entire **available** data spectrum. The linear regression determines the
 396 usual duration of the selected precipitation event. Subsequently, an hour is randomly selected for the
 397 start of the precipitation event. A goal of Teddy was to consider the physical consistency of inter-
 398 variable relationships. Precipitation generally affects other climate variables (e.g. humidity, radiation,

- hat gelöscht: failing
- hat gelöscht: see
- hat gelöscht: ure
- hat gelöscht: ?
- hat formatiert: Nicht Hervorheben
- hat formatiert: Nicht Hervorheben
- hat formatiert: Nicht Hervorheben
- hat gelöscht:
- hat gelöscht: this doesn't help
- hat formatiert: Schriftfarbe: Automatisch

405 [temperature, etc.; Meredith et al., 2021](#)). During night, physical interdependencies between
406 precipitation and other variables are generally lower, because radiation is not affected and less energy
407 is available to affect other variables. This might have an effect for impact models, because, as an
408 example, evapotranspiration might be unrealistically high if precipitation occurs at the same time with
409 full solar irradiation during noon. In order to reduce possible inconsistencies with other variables that
410 could lead to implications in impact models, the precipitation is only distributed to hours at nighttime,
411 Alternatively, we implemented the option for the user to write Not a Number (NaN) values instead.

hat gelöscht: physical

hat gelöscht: (without solar radiation)

412 Drizzle precipitation (values below 1 mm day⁻¹) is also disaggregated to sub-daily values in order to
413 ensure mass and energy conservation. If no historical precipitation event is found for this case,
414 precipitation noise is again randomly distributed to an hour at nighttime. If no hour without radiation
415 occurs (e.g. high latitudes in northern summer), the precipitation is distributed to local midnight.

hat gelöscht: “

hat gelöscht: bias”

hat gelöscht: Precipitation

hat gelöscht:

hat gelöscht: are

hat gelöscht: !

416 The calculation procedure can be performed either for universal time (UT) or for local solar time (LST).
417 The latter divides the world into equal time zones of 15° with the central time zone (+7.5°) at
418 Greenwich.

419 4. Results

hat formatiert: Schriftart: Fett

420 In a first step, Teddy is applied for 30 globally distributed samples (Fig. 2) for the year 2010. To be able
421 to validate the results, we perform a cross-validation. Therefore, WFDE5 data for 2010 aggregated to
422 daily values serve as an input for Teddy. The same year is excluded from the statistical population
423 during the cross-validation. As a result, it can be tested how well WFDE5 hourly values for the year
424 2010 are reproduced with the statistical population of the other 39 years. The 30 samples are chosen
425 to represent globally relevant agricultural production regions in different climate zones (Fig. 2). To
426 evaluate the sensitivity of the different DOY window sizes, we run the cross-validation with different
427 DOY window sizes, ranging from 1 to 25, in steps of two, including the option to disable the DOY
428 window (DOY window size = 0). In order to additionally validate the performance for extreme events,
429 we perform a second cross-validation for all available 40 years (1980-2019) with DOY window sizes of
430 11 for sample location 29, located in Southern Germany.

Formatiert: Listenabsatz, Nummerierte Liste + Ebene: 1
+ Nummerierungsformatvorlage: 1, 2, 3, ... + Beginnen
bei: 1 + Ausrichtung: Links + Ausgerichtet an: 0,63 cm +
Einzug bei: 1,27 cm

hat nach unten verschoben [1]: Validation ¶

hat gelöscht: In a first step, a cross-validation is carried out
for 30 globally distributed samples (Fig. 2) for the year 2010.

hat formatiert: Schriftart: Fett

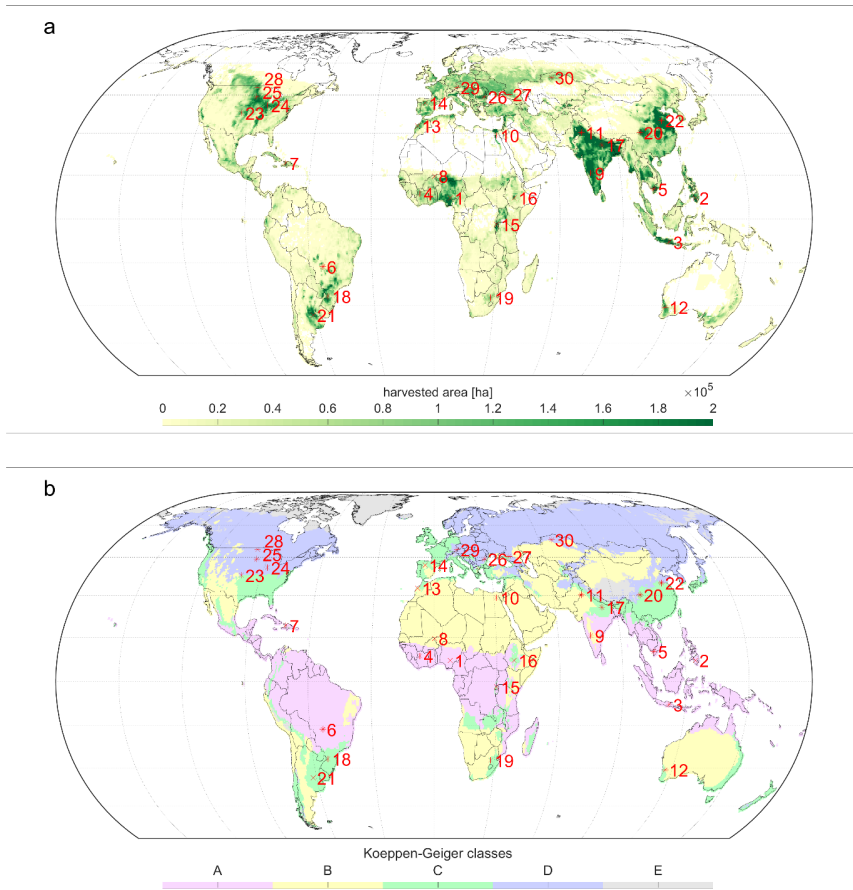
hat gelöscht: s

hat gelöscht: basic population

hat gelöscht: basic population

hat gelöscht: all

hat gelöscht: and 25



447

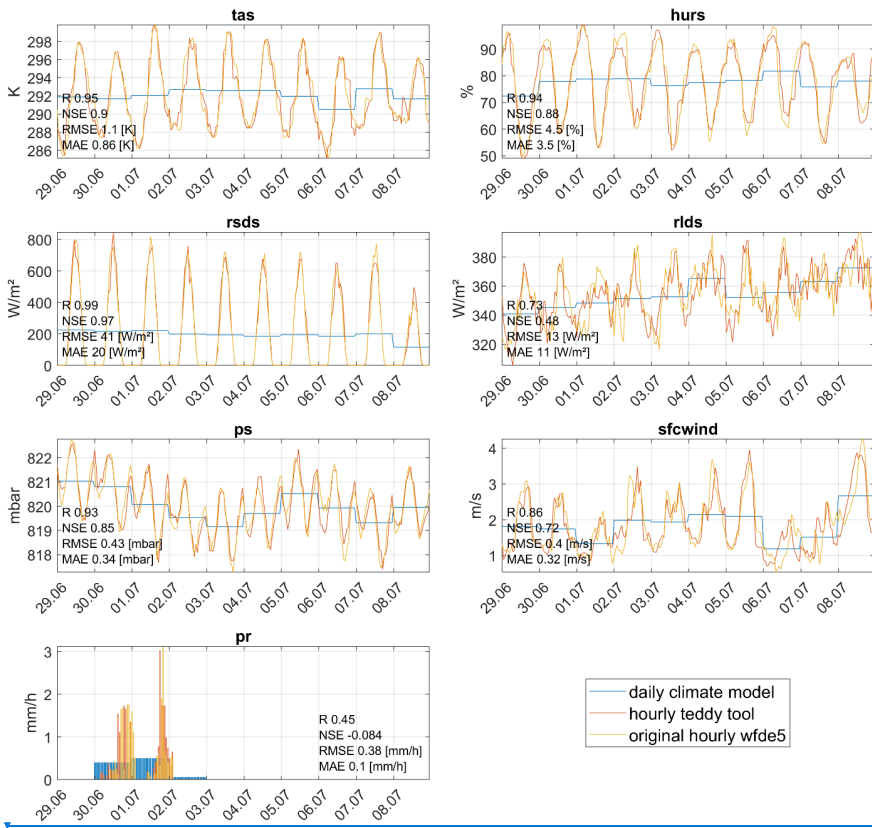
448

449 Figure 2: Distribution of 30 global samples used for the cross-validation on (a) annual total harvested
 450 area of rainfed and irrigated crops in hectare per pixel at a 30 arc-minute grid (Portmann et al., 2010)
 451 and (b) for Koeppen-Geiger climate zones calculated for 1980-2019 WFDE5 temperature and
 452 precipitation values (Beck et al., 2018). Samples are ordered by climate zone affiliation and their
 453 distance to the equator.

454 4.1 Validation

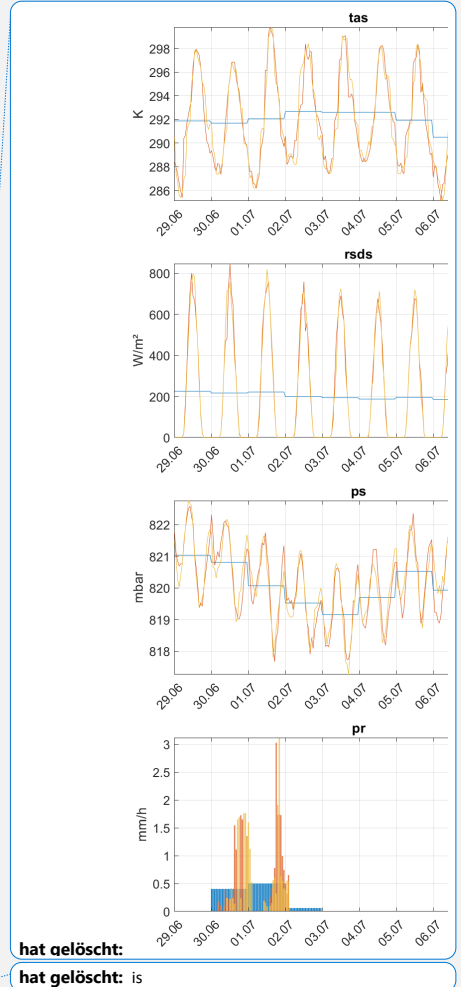
455 As an example, for sample location 16 in Ethiopia, Fig. 3 shows the results of the temporal
 456 disaggregation series for the cross-validation for a 10-day time series in 2010 in comparison with the
 457 daily climate input and the original hourly WFDE5 data. The hourly courses show high correlations for
 458 the randomly selected time series for all variables except for precipitation (Fig. 3 and scatterplots in
 459 Fig. 4 for the entire year; [Supplementary Fig. S2 and S3 alternatively show sample location 22 in China](#)).

- hat verschoben (Einfügung) [1]
- hat formatiert: Schriftart: Nicht Fett, Unterstrichen
- hat gelöscht: example



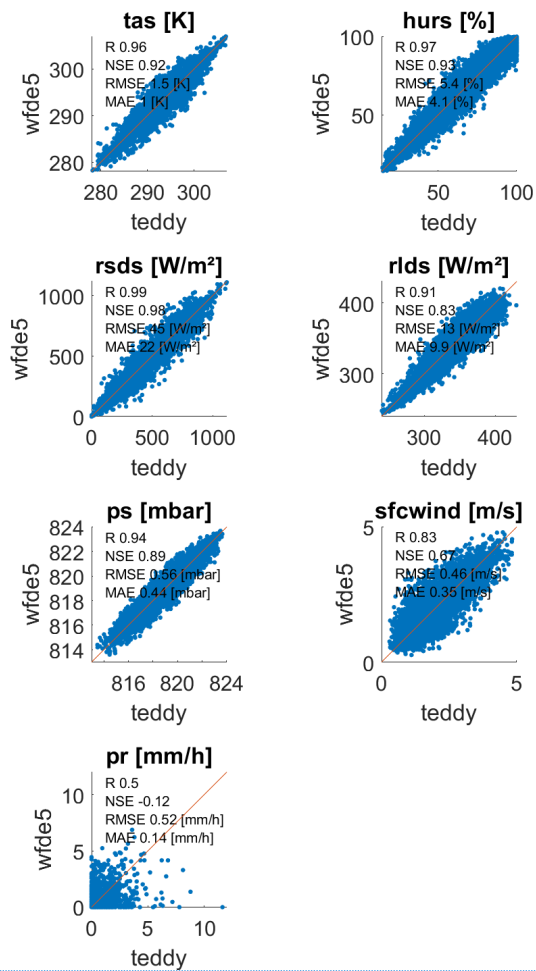
461

462 Figure 3: Time-series for all variables comparing daily climate model data, disaggregated hourly results
 463 of Teddy from the performed cross-validation and the original hourly WFDE5 data, shown for sample
 464 location 16 in Ethiopia with a DOY window size of 7 for the 10-day period 29.06. – 08.07.2010. The
 465 Pearson correlation coefficient (R), the Nash-Sutcliffe model efficiency coefficient (NSE), the root mean
 466 squared error (RMSE) and the mean absolute error (MAE) are displayed for the shown time period for
 467 each variable.



hat gelöscht:

hat gelöscht: is



470

471 Figure 4: Hourly values for the year 2010 between disaggregated values generated by the Teddy-Tool
 472 and the original WFDE5 data used for the cross-validation, exemplarily for sample [location](#) 16 in
 473 Ethiopia with a DOY window size of 7. [The Pearson correlation coefficient \(R\), the Nash-Sutcliffe model](#)
 474 [efficiency coefficient \(NSE\), the root mean squared error \(RMSE\) and the mean absolute error \(MAE\)](#)
 475 [are displayed for each variable.](#)

476 [4.2 Sensitivity analysis DOY window size](#)

477 The sensitivity analysis averaged over all 30 samples shows that the Pearson correlation coefficient of
 478 hourly values for the year 2010 show high correlations for all variables ($r > 0.9$), except wind_speed
 479 ($r > 0.7$) and precipitation ($r > 0.4$), which are generally more difficult to disaggregate (Fig. 5;
 480 [Supplementary Fig. S4 additionally shows the Nash-Sutcliffe model efficiency coefficient](#)). The selected
 481 DOY window size has an effect on the quality of the results. While no DOY window (size=0) results in

hat gelöscht: ¶

hat formatiert: Unterstrichen

Formatiert: Standard, Keine Aufzählungen oder Nummerierungen

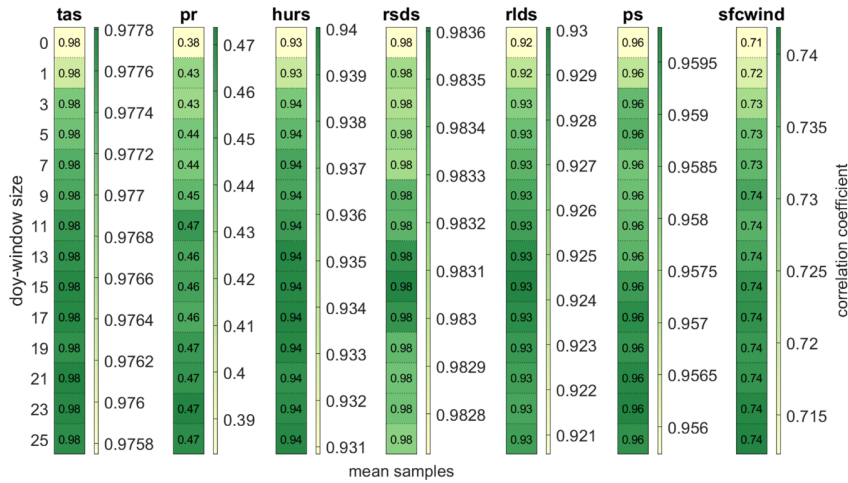
hat gelöscht: are the most difficult variables for disaggregation...

hat gelöscht:).

486 the lowest correlation coefficient across all variables, the DOY window size does significantly affect the
 487 correlation for precipitation and wind speed (Fig. 5).

hat gelöscht: not

hat gelöscht: except



488

489 Figure 5: Pearson correlation coefficient between disaggregated hourly values generated by the Teddy-
 490 Tool and the original WFDE5 data used for the cross-validation for different DOY window sizes
 491 averaged over all 30 samples for the year 2010 for all variables. The scaling of the colorbar differs
 492 between variables.

hat gelöscht: being disaggregated to hourly values

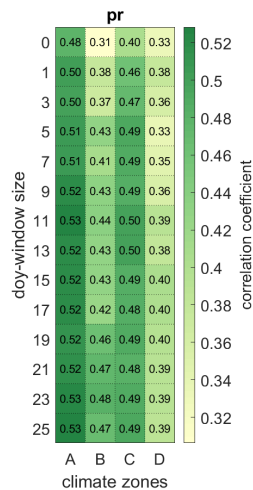
hat formatiert: Schriftart: 11 Pt.

493 For precipitation, the impact of the DOY window size on the correlation varies between regions. Larger
 494 DOY windows are mainly beneficial for precipitation in arid regions, while showing lower increases in
 495 correlation in regions with pronounced seasons (Fig. 6). The results also show that the correlation for
 496 precipitation is generally larger in tropical regions than in continental regions.

hat gelöscht: tropical and

hat gelöscht:

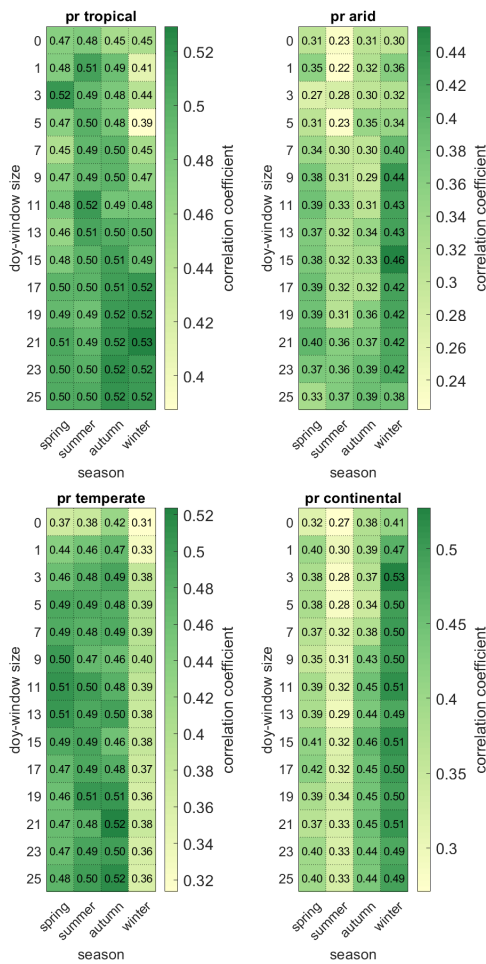
hat gelöscht: , the correlation might decrease with larger DOY window size...



497

505 Figure 6: Pearson correlation coefficient [between disaggregated hourly values generated by the Teddy-](#)
 506 [Tool and the original WFDE5 data used for the cross-validation](#) for different DOY window sizes
 507 averaged over the samples for each Koeppen-Geiger climate zone (A=tropical, B=arid, C=temperate,
 508 D=continental).

509 While hourly precipitation can be best reproduced for winter seasons in continental and arid regions,
 510 winter seasons show the lowest correlation for temperate regions. Tropical regions only show
 511 relatively low variations over the year, independently from the selected DOY window size (Fig. 7).
 512 Especially in arid regions, the length of the DOY window size affects the results differently in different
 513 seasons. Here, larger DOY windows decrease the correlation during the rainy season (winter and
 514 spring), while correlation is increased during the dry season (summer and autumn).



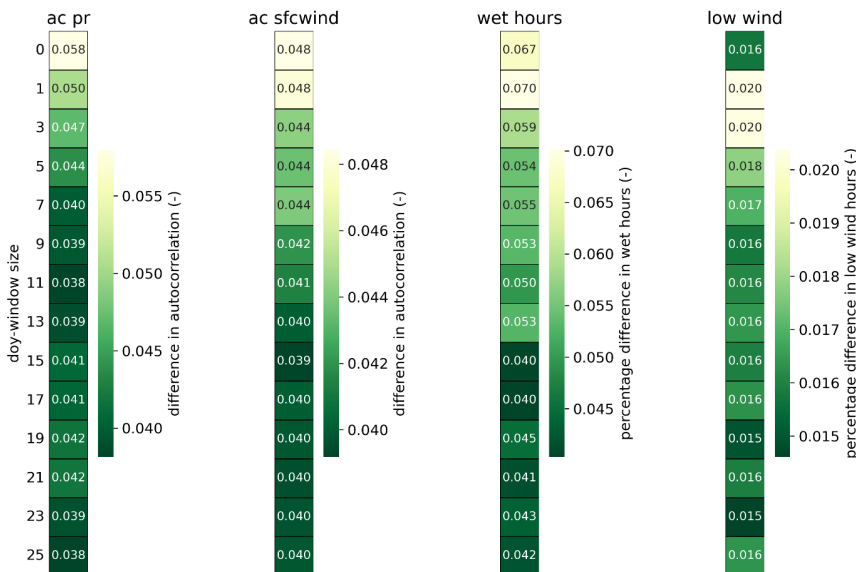
515

516 Figure 7: Pearson correlation coefficient [between disaggregated hourly values generated by the Teddy-](#)
 517 [Tool and the original WFDE5 data used for the cross-validation](#) for different DOY window sizes
 518 averaged over the samples for the four seasons ([Northern hemisphere: spring=MAM, summer=JJA,](#)
 519 [autumn=SON, winter=DJF; Southern hemisphere: spring=SON, summer=DJF, autumn= MAM,](#)
 520 [winter=JJA](#)). The heatmap is averaged over the samples for each Koeppen-Geiger climate zone
 521 (A=tropical, B=arid, C=temperate, D=continental).

hat gelöscht: The shift of the seasons between Northern and Southern hemisphere is considered.

522 Furthermore, we evaluate the sensitivity of the DOY window size to the reproduction of temporal
 523 autocorrelation (Fig. 8). Therefore, the autocorrelation over lag times between one and 24 hours is
 524 calculated for precipitation and wind speed. Autocorrelation refers to the similarity of a time series to
 525 a lag duration shifted version of the same time series. This allows sub-daily patterns and inter-hour
 526 connectivity to be statistically captured and validated in time series of precipitation and wind speed.
 527 In addition, we also check the reproduction of wet hours (precipitation above 0.1 mm h^{-1}) in 2010 and
 528 the number of hours with low wind speeds ($\text{sfcwind} < 2.5 \text{ m s}^{-1}$) referring to the typical cut-in wind
 529 speed of wind turbines.

530 Here, we find that short DOY window sizes below 5 days are not beneficial to all statistics. The
 531 autocorrelation of precipitation (wind speed) is reproduced more accurately with window sizes of 9
 532 days or longer. The number of wet hours is better recreated with window sizes above 15 days. For
 533 hours with low wind speed, a minor improvement is found above 9 days.



534

535 Figure 8: Extended validation statistics for the sensitivity analysis of the DOY window size for the year
 536 2010. The difference in autocorrelation refers to the average over all 30 [samples](#) and lag durations
 537 between one and 24 hours. Wet hours are defined as precipitation intensities above 0.1 mm h^{-1} and
 538 low wind speeds refer to hours with $\text{sfcwind} < 2.5 \text{ m s}^{-1}$.

hat gelöscht: stations

hat gelöscht: mm h^{-1}

hat gelöscht: m s^{-1}

544 4.3 Multi-year evaluation

545 The previous validation has assessed the disaggregation performance for all sample locations for the
546 year 2010 and different DOY window sizes. For the analysis of the whole time period 1980 – 2019, we
547 evaluate each year of the 40-year timeseries for sample location 29 and a window size of 11 days.
548 Figure 9 and Supplementary Fig. S5 show, the correlation coefficient and mean absolute error,
549 respectively, for each year to assess the interannual variability of disaggregation performance. For tas,
550 hurs, rlds, rlds, and ps the performance shows only very minor differences, whereas sfcwind and pr
551 show a higher degree of interannual fluctuations.

hat gelöscht: ¶

¶
¶
¶

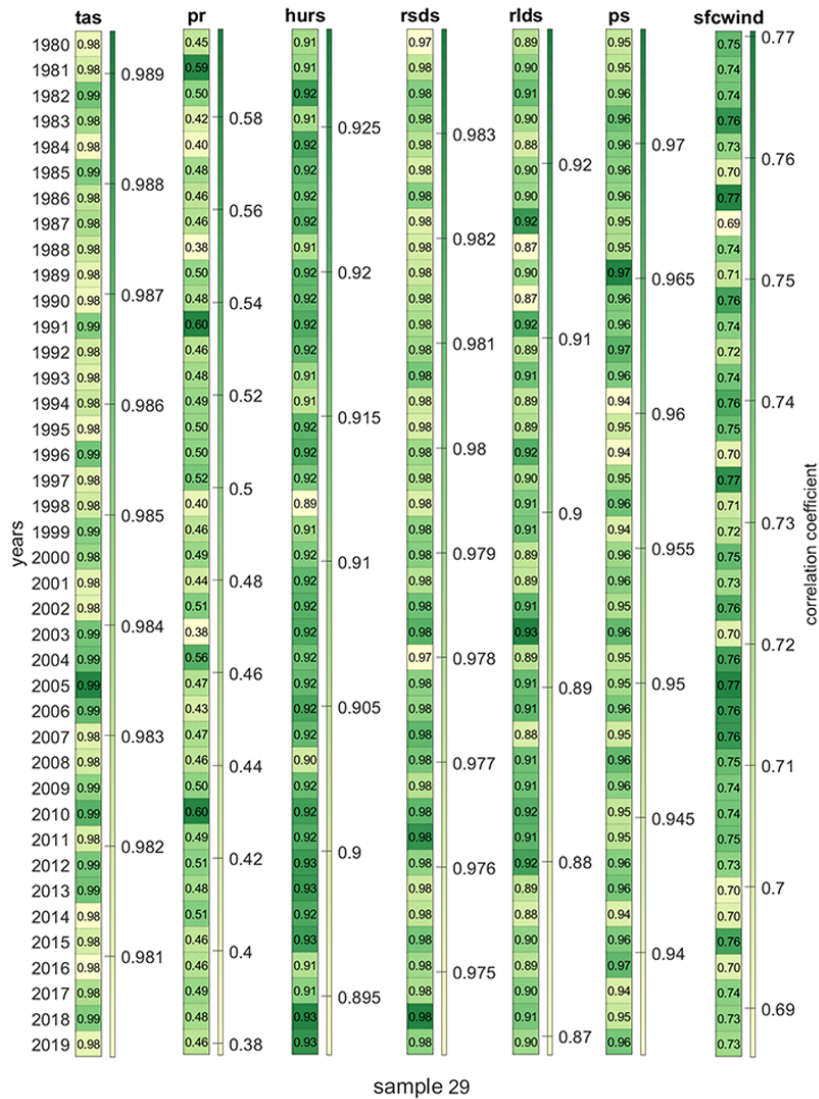
hat gelöscht: Evaluation of the whole period 1980 – 2019

hat gelöscht: ¶

hat gelöscht: s

hat gelöscht: the

hat gelöscht:



Formatiert: Zentriert

hat gelöscht: 98

hat gelöscht: Figure 9:

hat formatiert: Schriftart: 11 Pt., Nicht Kursiv, Schriftfarbe: Automatisch

hat formatiert: Schriftart: 11 Pt., Nicht Kursiv, Schriftfarbe: Automatisch

Feldfunktion geändert

hat gelöscht: -

hat gelöscht: ¶

¶

hat formatiert: Unterstrichen

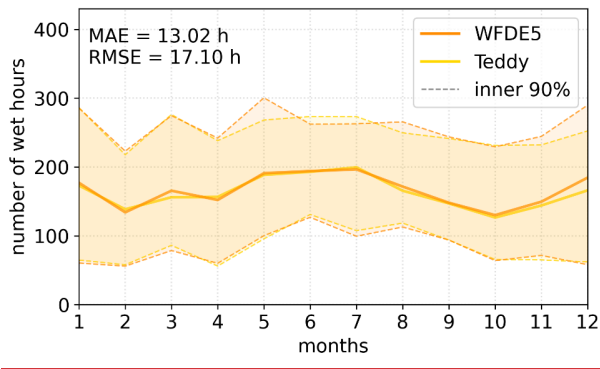
562

563 [Figure 9: Pearson correlation coefficient between disaggregated hourly values generated by the Teddy-](#)
 564 [Tool and the original WFDE5 data used for the cross-validation for each year from 1980 to 2019 for](#)
 565 [sample location 29 and a DOY window size of 11 days. The scaling of the colorbar differs between](#)
 566 [variables.](#)

567 [4.4 Evaluation of precipitation: Wet proportions and intensities](#)

574 For the further evaluation of precipitation characteristics, we additionally assess the disaggregated
 575 timeseries over the whole period 1980 – 2019 for sample location 29. In order to evaluate the
 576 reproduction of wet/dry proportions, the monthly cycle of wet hours is provided (Fig. 10). Wet hours
 577 above 0.1 mm h^{-1} are recreated by the Teddy-Tool with minor differences for the median over 40 years
 578 (Fig. 10). The error measures are calculated for every year separately amounting to a mean absolute
 579 error of 13.02 h equaling 7.8 %.

580 For the evaluation of the range of precipitation intensities, Fig. 11 shows intensities above 1 mm h^{-1}
 581 plotted against its percentage of exceedance for sub-daily durations. We find that the disaggregated
 582 precipitation intensities match the original data except for extreme precipitation.



583
 584 Figure 10: Number of wet hours per month for sample location 29 in Germany. Solid lines show the
 585 median over 40 years, where the dashed lines denote the inner 90% of the 40-year period. MAE and
 586 RMSE are calculated separately for every year and averaged over 40 years.

hat gelöscht: also

hat gelöscht: is assessed

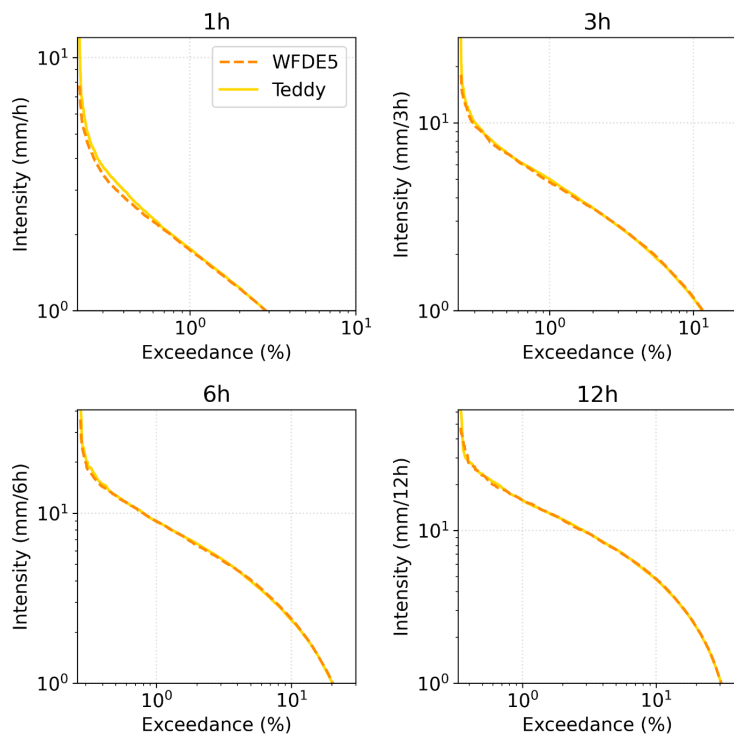
hat gelöscht: ure

hat gelöscht: ¶

Formatiert: Zentriert

hat gelöscht: 109

hat gelöscht: Figure 10:



595

596 [Figure 11: Exceedance probability of precipitation intensities for sub-daily durations for sample](#)
 597 [location 29 in Germany.](#)

598 [4.5 Evaluation of precipitation extremes](#)

599 As the ISIMIP data base is used for future impact modelling and historical attribution science (Mengel
 600 et al., 2021), extremes are of major interest for the community. The ability of global climate models to
 601 simulate sub-daily extremes is limited and depends on the variable of interest and the spatio-temporal
 602 conditions of the extreme and the respective model setup (Wehner et al., 2021; Kumar et al., 2015;
 603 Wang and Clow, 2020). However, in this validation, we evaluate how the Teddy-Tool is able to preserve
 604 the statistics of sub-daily extreme values. Therefore, we select precipitation as variable of interest.

605 Figure 12 shows the reproduction of sub-daily precipitation extremes for 1980 – 2019 for sample
 606 location 29 in southern Germany, where Teddy is run with a DOY window size of 11 days. The 40 annual
 607 maxima are extracted from the original and the disaggregated data. Additionally, the Generalized
 608 Extreme Value (GEV) distribution is fitted to these empirical data. [GEV parameters are estimated via](#)
 609 [Maximum Likelihood Estimation \(Coles, 2001\), where the goodness-of-fit is assessed with the](#)
 610 [Anderson-Darling test at 95% significance level \(Stephens, 1986\).](#) Thereby, 95% confidence intervals
 611 are generated applying a bootstrap procedure with 1000 iterations to account for extreme value
 612 statistical uncertainties. We find that the Teddy-Tool leads to an overestimation of annual maximum
 613 precipitation. For the hourly duration, the differences are large with the confidence intervals of the

Formatiert: Zentriert, Nicht vom nächsten Absatz trennen

hat gelöscht: 119

hat gelöscht: 11

hat formatiert: Schriftart: Nicht Kursiv

hat formatiert: Schriftart: Nicht Kursiv

hat formatiert: Schriftart: Nicht Kursiv

hat formatiert: Schriftart: Nicht Kursiv

hat gelöscht: ¶

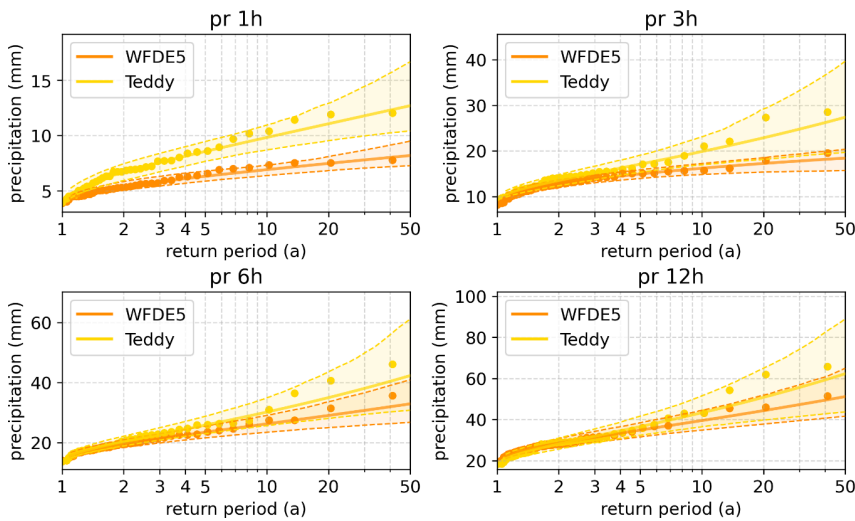
hat formatiert: Unterstrichen

hat gelöscht: need to

hat gelöscht: 1

hat gelöscht:

620 GEV hardly overlapping. For the longer durations, Teddy values approach the original data, with
 621 noticeable differences only for the rare events with return periods above 5 years.



622

623 Figure 12: Extreme value statistical evaluation of sub-daily precipitation for sample location 29 in
 624 Germany. The annual maxima of the WFDE5 and Teddy are shown as dots. Additionally, GEV fits (lines)
 625 with 95% confidence intervals (transparent areas and dashed lines) account for uncertainties. The
 626 Teddy-Tool is run with a DOY window size of 11 days.

627 **5. Discussion and Outlook**

628 The Teddy-Tool allows for temporal disaggregation of daily climate model data. The disaggregation is
 629 based on location and time specific empirical relationships between variables. The approach is well
 630 suitable for all tested variables and results in very high correlations (>0.9), except for precipitation
 631 (>0.5) and wind speed (>0.75). We refer the worse performance for precipitation and wind speed to
 632 the high intra-day variability for these variables (Watters et al., 2021). Other variables are governed by
 633 a stronger diurnal cycle (Dai and Trenberth, 2004), which is easier to disaggregate based on empirical
 634 diurnal profiles.

635 Compared to other approaches, the advantage of the Teddy-Tool is that no other input data is required
 636 rather than the daily climate model data. The Teddy-Tool is relatively simple to apply, considers specific
 637 local and seasonal features of the diurnal course of different climate variables, and preserves the
 638 physical consistency of inter-variable relationships. Mass and energy are conserved and mean daily
 639 values of the climate model are reproduced any time.

640 The spatial and temporal resolution of the results is determined by the provided temporal and spatial
 641 resolution of the chosen reference data (WFDE5 used here). Longer available reanalysis time periods
 642 extend the statistical population for identifying the most similar weather conditions in the past and
 643 thus could improve the results. Generally, also other reference data could be used, that provides higher
 644 temporal or spatial resolution for a specific region.

hat gelöscht: 129

hat gelöscht: Figure 29:

hat gelöscht: ¶

hat gelöscht: Conclusions

hat formatiert: Schriftart: Fett

Formatiert: Nummerierte Liste + Ebene: 1 + Nummerierungsformatvorlage: 1, 2, 3, ... + Beginnen bei: 1 + Ausrichtung: Links + Ausgerichtet an: 0,63 cm + Einzug bei: 1,27 cm

hat gelöscht: er

hat gelöscht: The o

hat gelöscht: regional

hat gelöscht: considers

hat gelöscht:

hat gelöscht: basic population

655 The DOY window to find the most similar historical weather situations can be chosen in different sizes.
656 For most of the variables, we found small effects of time window adjustments, except for precipitation
657 and wind speed. The evaluation of different DOY window sizes reveals that a DOY window size of 11
658 can generally be recommended across all variables. Larger DOY windows should be avoided mainly in
659 arid regions, while shorter DOY windows generally lead to poorer representations of autocorrelation
660 and extreme events.

hat gelöscht: time

661 One limitation of the Teddy-Tool is the representation of extreme events, mainly for precipitation,
662 which is generally the most difficult variable for temporal disaggregation. We found that hourly
663 precipitation extremes are overestimated. For heavy daily precipitation events, Teddy distributes the
664 24h-sums either correctly, too evenly or on too few hours. When distributing on too few hours,
665 extreme hourly intensities evolve, which may have never occurred or may even be physically
666 implausible. For temporal disaggregation of extreme precipitation, we recommend dynamical
667 downscaling via high-resolution climate models (Poschlod, 2021; Poschlod et al., 2021; Zabel et al.,
668 2012; Zabel and Mauser, 2013).

hat gelöscht:

hat gelöscht: not always reproduced

669 Another limitation of the approach is the reproduction of the inter-day connectivity within the
670 disaggregated time series. When two diurnal profiles are chosen for the disaggregation of adjacent
671 days, which show dissimilar courses in the time steps at the change of the day, abrupt value jumps
672 might occur in the disaggregation. This can be seen in Fig. 3 for rlds from July 4th to July 5th. To illustrate
673 this issue, a disaggregation time series from another location is provided in Supplementary Fig. S2. This
674 limitation does also apply for the Method of Fragments applied on precipitation (Li et al., 2018).
675 Similarly to Li et al. (2018), we also consider the precipitation state of the previous and following day
676 to improve inter-day connectivity. Without this additional consideration, overnight precipitation
677 events would often be 'cut off' in the disaggregation. For the remaining abrupt jumps in the
678 disaggregated time series, we refrain from post-processing with subsequent smoothing, as we want to
679 preserve both mass and energy and the empirical diurnal profiles.

hat gelöscht:

hat gelöscht: 4

hat gelöscht: 5

hat formatiert: Hochgestellt

hat formatiert: Hochgestellt

hat gelöscht: the

hat gelöscht: ure

hat gelöscht: 2

hat gelöscht: "

hat gelöscht: "

hat gelöscht:

680 For the disaggregation of future climate projections using of the Teddy-Tool, we have the following
681 remarks: As the Teddy-Tool derives the relationships between sub-daily and daily values empirically
682 based on reanalysis data, future diurnal profiles, which are outside the historical range of diurnal
683 profiles, might possibly be not fully reproduced. However, this limitation is common for statistical
684 approaches, which are to be calibrated on historical data (Papalexou et al., 2018). Nevertheless, due
685 to energy and mass conservation, climate trends in the daily climate signal are fully preserved. Hence,
686 applying Teddy for temporal disaggregation under climate change holds under the assumption that we
687 select the most similar meteorological day of the historical data and that this diurnal profile is
688 representative for future climatic conditions. However, this assumption might apply to a different
689 degree for different variables. We expect non-stationarity for the diurnal profiles due to changing
690 weather patterns, shifts in rainfall generating processes, and shifts in the seasonality, mainly for
691 precipitation and wind. The daily course of other variables, such as solar radiation and temperature
692 might generally be less affected by a warmer climate. Furthermore, global climate models at coarse
693 resolutions generally do not represent all processes to fully reproduce intra-day variability. Teddy
694 applies the diurnal profiles and intra-day variability from the WFDE5 data, which are bias-adjusted
695 ERA5 reanalysis data that implicitly consider finer scale effects than coarse-resolution global climate
696 models (Cucchi et al., 2020). Thus, the disaggregation process in Teddy is consistent with the bias
697 adjustment in ISIMIP3.

710 Another limitation of the methodology could occur in the case of strong climate change signals. In case
711 of high warming in end-of-century projections, the number of sampled historical days might decrease
712 if the same historical day is sampled repeatedly. This could lead to reductions in diversity of the diurnal
713 profile. Hence, Teddy allows to monitor the number of unique analogue days per year. An additional
714 analysis for SSP3-7.0 using the GFDL-ESM4 climate model shows that the number of unique analogue
715 climate days are declining, as expected, but still the diversity of chosen days is above 300 unique days
716 at the end of the century for a chosen moving-window size of +11 days (Supplementary Fig. S6). A
717 smaller size of the moving window prevents that the same analogue day is chosen over a longer time
718 period. This will increase the diversity of diurnal profiles at the expense of similarity. Even if diurnal
719 profiles are derived from the same analogue day repeatedly, the disaggregated diurnal courses, e.g.
720 for temperature, will show variations (different offset and different amplitude) due to conservation of
721 daily mean energy and mass. From a broader perspective, it is also not clear whether the uncertainties
722 resulting from this limitation are larger than the uncertainties within the climate model projections
723 until the end of the century. Furthermore, in the long term, the basic population for finding analogue
724 climates will continuously increase, since WFDE5 data, which are based on ERA5, are continuously
725 updated. We note that Teddy could be also employed to disaggregate future daily climate projections
726 based on hourly future climate projections as reference.

727 Further possible developments could include improvements for the reproduction of the inter-day
728 connectivity. Despite the consideration of precipitation classes, still abrupt value jumps over day
729 changes are possible. A future introduction of temperature classes and surface pressure classes in
730 addition to the precipitation classes could help to reduce this effect. Depending on the location of
731 interest, also including climate modes or weather patterns for the choice of the most similar
732 meteorological day could positively affect the performance. Furthermore, depending on the
733 application, it could be reasonable not to screen for the most similar meteorological day, but for the
734 most similar succession of multiple days. This would as a consequence improve the inter-day
735 connectivity as less different profiles are selected.

736 Other optional future developments could include the separation of direct and diffuse radiation, which
737 is also a required information for some impact models which is currently not provided by ISIMIP.
738 However, we would make further development with more options dependent on the community's
739 adoption of the current executable tool.

740 Code availability

741 The source code of the Teddy-Tool (v1.1) and a parallelized version of the Teddy-Tool (v1.1p), including
742 a precompiled executable file for Windows, preprocessed data, results of the cross-validation and
743 exemplary results for SSP 585 (2015 – 2100) and the UKESM1-0-L climate model for 30 samples are
744 provided via Zenodo (<https://doi.org/10.5281/zenodo.8124111>).

745 Author contribution

746 FZ: Conceptualization, Software, Methodology, Validation, Formal analysis, Resources, Data curation,
747 Writing - original draft, Visualization

748 BP: Methodology, Validation, Formal analysis, Writing - original draft, Visualization

749 Competing interests

Formatiert: Standard

hat gelöscht: In order to prevent for high warming

hat gelöscht: that

hat gelöscht: , which

hat formatiert: Nicht Hervorheben

hat formatiert: Nicht Hervorheben

hat formatiert: Nicht Hervorheben

hat gelöscht:

hat formatiert: Nicht Hervorheben

hat formatiert: Nicht Hervorheben

hat formatiert: Nicht Hervorheben

hat formatiert: Schriftfarbe: Automatisch

hat gelöscht: Since mass and energy are conserved within the disaggregation approach, the

hat gelöscht: might

hat gelöscht: despite the diurnal profile are derived from the same analogue day

hat gelöscht:

hat gelöscht: an improved

hat gelöscht: changes

hat gelöscht: improve

hat gelöscht: 0

Formatiert: Block

hat gelöscht: 10.5281/zenodo.7679149

765 The contact author has declared that none of the authors has any competing interests.

766 Acknowledgements

767 We acknowledge the methodological discussion with Stefan Lange from the Potsdam Institute of
768 Climate Impact Research (PIK).

769 References

- 770 Ailliot, P., Allard, D., Monbet, V., and Naveau, P.: Stochastic weather generators: an overview of
771 weather type models, *Journal de la société française de statistique*, 156, <https://doi.org/101-113>,
772 2015.
- 773 Beck, H. E., Zimmermann, N. E., McVicar, T. R., Vergopolan, N., Berg, A., and Wood, E. F.: Present and
774 future Köppen-Geiger climate classification maps at 1-km resolution, *Scientific Data*, 5, 180214,
775 <https://doi.org/10.1038/sdata.2018.214>, 2018.
- 776 [Bennett, A., Hamman, J. & Nijsen, B.: MetSim: A python package for estimation and disaggregation
777 of meteorological data, *Journal of Open Source Software*, 5\(47\), 2042,
778 <https://doi.org/10.21105/joss.02042>, 2020.](https://doi.org/10.21105/joss.02042)
- 779 Breinl, K. and Di Baldassarre, G.: Space-time disaggregation of precipitation and temperature across
780 different climates and spatial scales, *Journal of Hydrology: Regional Studies*, 21, 126-146,
781 <https://doi.org/10.1016/j.ejrh.2018.12.002>, 2019.
- 782 Buck, A. L.: New Equations for Computing Vapor Pressure and Enhancement Factor, *Journal of*
783 *Applied Meteorology and Climatology*, 20, 1527-1532, [https://doi.org/10.1175/1520-
784 0450\(1981\)020<1527:Nefcvp>2.0.Co;2](https://doi.org/10.1175/1520-0450(1981)020<1527:Nefcvp>2.0.Co;2), 1981.
- 785 Byers, E., Gidden, M., Leclère, D., Balkovic, J., Burek, P., Ebi, K., Greve, P., Grey, D., Havlik, P., Hillers,
786 A., Johnson, N., Kahil, T., Krey, V., Langan, S., Nakicenovic, N., Novak, R., Obersteiner, M.,
787 Pachauri, S., Palazzo, A., Parkinson, S., Rao, N. D., Rogelj, J., Satoh, Y., Wada, Y., Willaarts, B., and
788 Riahi, K.: Global exposure and vulnerability to multi-sector development and climate change
789 hotspots, *Environmental Research Letters*, 13, 055012, [https://doi.org/10.1088/1748-
790 9326/aabf45](https://doi.org/10.1088/1748-9326/aabf45), 2018.
- 791 Chen, D., Dai, A., and Hall, A.: The Convective-To-Total Precipitation Ratio and the “Drizzling” Bias in
792 Climate Models, *Journal of Geophysical Research: Atmospheres*, 126, e2020JD034198,
793 <https://doi.org/10.1029/2020JD034198>, 2021.
- 794 [Chen, C. J.: Temporal disaggregation of seasonal forecasting for streamflow simulation. *World
795 Environmental and Water Resources Congress 2016*, pp. 63-72, 2016.](https://doi.org/10.1007/978-1-4471-3675-0)
- 796 [Coles, S.: *An Introduction to Statistical Modeling of Extreme Values*. Springer, London, U.K.
797 <https://doi.org/10.1007/978-1-4471-3675-0>, 2001.](https://doi.org/10.1007/978-1-4471-3675-0)
- 798 Colón-González, F. J., Sewe, M. O., Tompkins, A. M., Sjödin, H., Casallas, A., Rocklöv, J., Caminade, C.,
799 and Lowe, R.: Projecting the risk of mosquito-borne diseases in a warmer and more populated
800 world: a multi-model, multi-scenario intercomparison modelling study, *The Lancet Planetary
801 Health*, 5, e404-e414, [https://doi.org/10.1016/S2542-5196\(21\)00132-7](https://doi.org/10.1016/S2542-5196(21)00132-7), 2021.
- 802 Cucchi, M., Weedon, G. P., Amici, A., Bellouin, N., Lange, S., Müller Schmied, H., Hersbach, H., and
803 Buontempo, C.: WFDE5: bias-adjusted ERA5 reanalysis data for impact studies, *Earth Syst. Sci.
804 Data*, 12, 2097-2120, <https://doi.org/10.5194/essd-12-2097-2020>, 2020.
- 805 [Dai, A. and Trenberth, K. E.: The Diurnal Cycle and Its Depiction in the Community Climate System
806 Model. *Journal of Climate*, 17, 930-951, \[https://doi.org/10.1175/1520-
807 0442\\(2004\\)017<0930:TDCAID>2.0.CO;2\]\(https://doi.org/10.1175/1520-0442\(2004\)017<0930:TDCAID>2.0.CO;2\), 2004.](https://doi.org/10.1175/1520-0442(2004)017<0930:TDCAID>2.0.CO;2)
- 808 Debele, B., Srinivasan, R., and Yves Parlange, J.: Accuracy evaluation of weather data generation and
809 disaggregation methods at finer timescales, *Advances in Water Resources*, 30, 1286-1300,
810 <https://doi.org/10.1016/j.advwatres.2006.11.009>, 2007.
- 811 Degife, A. W., Zabel, F., and Mauser, W.: Climate change impacts on potential maize yields in
812 Gambella region, Ethiopia, *Regional Environmental Change*, [https://doi.org/10.1007/s10113-021-
813 01773-3](https://doi.org/10.1007/s10113-021-01773-3), 2021.

hat formatiert: Absatz-Standardschriftart

hat formatiert: Absatz-Standardschriftart

814 Eyring, V., Bony, S., Meehl, G. A., Senior, C. A., Stevens, B., Stouffer, R. J., and Taylor, K. E.: Overview
815 of the Coupled Model Intercomparison Project Phase 6 (CMIP6) experimental design and
816 organization, *Geosci. Model Dev.*, 9, 1937-1958, <https://doi.org/10.5194/gmd-9-1937-2016>, 2016.

817 Förster, K., Hanzer, F., Winter, B., Marke, T., and Strasser, U.: An open-source MEteoroLogical
818 observation time series DISaggregation Tool (MELODIST v0.1.1), *Geosci. Model Dev.*, 9, 2315-
819 2333, <https://doi.org/10.5194/gmd-9-2315-2016>, 2016.

820 Franke, J. A., Müller, C., Minoli, S., Elliott, J., Folberth, C., Gardner, C., Hank, T., Izaurralde, R. C.,
821 Jägermeyr, J., Jones, C. D., Liu, W., Olin, S., Pugh, T. A. M., Ruane, A. C., Stephens, H., Zabel, F., and
822 Moyer, E. J.: Agricultural breadbaskets shift poleward given adaptive farmer behavior under
823 climate change, *Global Change Biol.*, 28, 167-181, <https://doi.org/10.1111/gcb.15868>, 2022.

824 Golub, M., Thiery, W., Marcé, R., Pierson, D., Vanderkelen, I., Mercado-Bettin, D., Woolway, R. I.,
825 Grant, L., Jennings, E., Kraemer, B. M., Schewe, J., Zhao, F., Frieler, K., Mengel, M., Bogomolov, V.
826 Y., Bouffard, D., Côté, M., Couture, R. M., Debolskiy, A. V., Droppers, B., Gal, G., Guo, M., Janssen,
827 A. B. G., Kirillin, G., Ladwig, R., Magee, M., Moore, T., Perroud, M., Piccolroaz, S., Raaman Vinnaa,
828 L., Schmid, M., Shatwell, T., Stepanenko, V. M., Tan, Z., Woodward, B., Yao, H., Adrian, R., Allan,
829 M., Anneville, O., Arvola, L., Atkins, K., Boegman, L., Carey, C., Christianson, K., de Eyto, E.,
830 DeGasperi, C., Grechushnikova, M., Hejzlar, J., Joehnk, K., Jones, I. D., Laas, A., Mackay, E. B.,
831 Mammarella, I., Markensten, H., McBride, C., Özkundakci, D., Potes, M., Rinke, K., Robertson, D.,
832 Rusak, J. A., Salgado, R., van der Linden, L., Verburg, P., Wain, D., Ward, N. K., Wollrab, S., and
833 Zdorovenova, G.: A framework for ensemble modelling of climate change impacts on lakes
834 worldwide: the ISIMIP Lake Sector, *Geosci. Model Dev.*, 15, <https://doi.org/4597-4623>,
835 10.5194/gmd-15-4597-2022, 2022.

836 Görner, C., Franke, J., Kronenberg, R., Hellmuth, O., and Bernhofer, C.: Multivariate non-parametric
837 Euclidean distance model for hourly disaggregation of daily climate data, *Theoretical and Applied
838 Climatology*, 143, 241-265, <https://doi.org/10.1007/s00704-020-03426-7>, 2021.

839 Jägermeyr, J., Müller, C., Ruane, A. C., Elliott, J., Balkovic, J., Castillo, O., Faye, B., Foster, I., Folberth,
840 C., Franke, J. A., Fuchs, K., Guarin, J. R., Heinke, J., Hoogenboom, G., Iizumi, T., Jain, A. K., Kelly, D.,
841 Khabarov, N., Lange, S., Lin, T.-S., Liu, W., Mialyk, O., Minoli, S., Moyer, E. J., Okada, M., Phillips,
842 M., Porter, C., Rabin, S. S., Scheer, C., Schneider, J. M., Schyns, J. F., Skalsky, R., Smerald, A., Stella,
843 T., Stephens, H., Webber, H., Zabel, F., and Rosenzweig, C.: Climate impacts on global agriculture
844 emerge earlier in new generation of climate and crop models, *Nature Food*, 2, 873-885,
845 <https://doi.org/10.1038/s43016-021-00400-y>, 2021.

846 [Juckes, M., Taylor, K. E., Durack, P. J., Lawrence, B., Mizielinski, M. S., Pamment, A., Peterschmitt, J.-
847 Y., Rixen, M., and Sénési, S.: The CMIP6 Data Request \(DREQ, version 01.00.31\), *Geosci. Model
848 Dev.*, 13, 201-224, <https://doi.org/10.5194/gmd-13-201-2020>, 2020.](https://doi.org/10.5194/gmd-13-201-2020)

849 Kumar, D., Mishra, V., and Ganguly, A. R.: Evaluating wind extremes in CMIP5 climate models,
850 *Climate Dynamics*, 45, 441-453, <https://doi.org/10.1007/s00382-014-2306-2>, 2015.

851 Kunstmann, H. and Stadler, C.: High resolution distributed atmospheric-hydrological modelling for
852 Alpine catchments, *Journal of Hydrology*, 314, 105-124,
853 <https://doi.org/10.1016/j.jhydrol.2005.03.033>, 2005.

854 Lange, S.: Trend-preserving bias adjustment and statistical downscaling with ISIMIP3BASD (v1.0),
855 *Geosci. Model Dev.*, 12, 3055-3070, <https://doi.org/10.5194/gmd-12-3055-2019>, 2019.

856 Li, X., Meshgi, A., Wang, X., Zhang, J., Tay, S. H. X., Pijcke, G., Manocha, N., Ong, M., Nguyen, M. T.,
857 and Babovic, V.: Three resampling approaches based on method of fragments for daily-to-subdaily
858 precipitation disaggregation, *International Journal of Climatology*, 38, e1119-e1138,
859 <https://doi.org/10.1002/joc.5438>, 2018.

860 Liston, G. E. and Elder, K.: A Meteorological Distribution System for High-Resolution Terrestrial
861 Modeling (MicroMet), *Journal of Hydrometeorology*, 7, 217-234,
862 <https://doi.org/10.1175/jhm486.1>, 2006.

863 Liu, C., Ikeda, K., Thompson, G., Rasmussen, R., and Dudhia, J.: High-Resolution Simulations of
864 Wintertime Precipitation in the Colorado Headwaters Region: Sensitivity to Physics

865 Parameterizations, *Monthly Weather Review*, 139, 3533-3553, <https://doi.org/10.1175/MWR-D-11-00009.1>, 2011.

866

867 [Lüttgau, J., Kunkel, J.: Cost and Performance Modeling for Earth System Data Management and Beyond. In: Yokota, R., Weiland, M., Shalf, J., Alam, S. \(eds\) High Performance Computing. ISC High Performance 2018. Lecture Notes in Computer Science, vol 11203. Springer, Cham.](#)

868

869 https://doi.org/10.1007/978-3-030-02465-9_2, 2018.

870

871 Mengel, M., Treu, S., Lange, S., and Frieler, K.: ATTRICI v1.1 – counterfactual climate for impact attribution, *Geosci. Model Dev.*, 14, 5269-5284, <https://doi.org/10.5194/gmd-14-5269-2021>,

872

873 2021.

874 [Meredith, E., Ulbrich, U., Rust, H. W., and Truhetz, H.: Present and future diurnal hourly precipitation in 0.11° EURO-CORDEX models and at convection-permitting resolution, *Environmental Research Communications*, 3, 055002, <https://doi.org/10.1088/2515-7620/abf15e>, 2021.](#)

875

876

877 Mezghani, A. and Hingray, B.: A combined downscaling-disaggregation weather generator for stochastic generation of multisite hourly weather variables over complex terrain: Development and multi-scale validation for the Upper Rhone River basin, *Journal of Hydrology*, 377, 245-260, <https://doi.org/10.1016/j.jhydrol.2009.08.033>, 2009.

878

879

880 Minoli, S., Jägermeyr, J., Asseng, S., Urfels, A., and Müller, C.: Global crop yields can be lifted by timely adaptation of growing periods to climate change, *Nature Communications*, 13, 7079, <https://doi.org/10.1038/s41467-022-34411-5>, 2022.

881

882

883 Orlov, A., Daloz, A. S., Sillmann, J., Thiery, W., Douzal, C., Lejeune, Q., and Schleussner, C.: Global Economic Responses to Heat Stress Impacts on Worker Productivity in Crop Production, *Economics of Disasters and Climate Change*, 5, 367-390, <https://doi.org/10.1007/s41885-021-00091-6>, 2021.

884

885

886 Orlov, A., et al.: Human heat stress could offset economic benefits of the CO2 fertilisation effect in crop production. *Nature Communications: Under Review*, 2023.

887

888

889 Papalexioi, S. M., Markonis, Y., Lombardo, F., AghaKouchak, A., and Foufoula-Georgiou, E.: Precise Temporal Disaggregation Preserving Marginals and Correlations (DiPMaC) for Stationary and Nonstationary Processes, *Water Resources Research*, 54, 7435-7458, <https://doi.org/10.1029/2018WR022726>, 2018.

890

891

892

893 Park, H. and Chung, G.: A Nonparametric Stochastic Approach for Disaggregation of Daily to Hourly Rainfall Using 3-Day Rainfall Patterns, *Water*, 12, 2306, 2020.

894

895

896 Portmann, F. T., Siebert, S., and Döll, P.: MIRCA2000—Global monthly irrigated and rainfed crop areas around the year 2000: A new high-resolution data set for agricultural and hydrological modeling, *Global Biogeochemical Cycles*, 24, <https://doi.org/10.1029/2008GB003435>, 2010.

897

898

899 Poschlod, B.: Using high-resolution regional climate models to estimate return levels of daily extreme precipitation over Bavaria, *Nat. Hazards Earth Syst. Sci.*, 21, 3573-3598, <https://doi.org/10.5194/nhess-21-3573-2021>, 2021.

900

901

902 [Poschlod, B.: Attributing heavy rainfall event in Berchtesgadener Land to recent climate change – Further rainfall intensification projected for the future, *Weather Clim Extremes*, 38, 100492, <https://doi.org/10.1016/j.wace.2022.100492>, 2022.](#)

903

904

905 Poschlod, B. and Ludwig, R.: Internal variability and temperature scaling of future sub-daily rainfall return levels over Europe, *Environmental Research Letters*, 16, 064097, <https://doi.org/10.1088/1748-9326/ac0849>, 2021.

906

907

908 Poschlod, B., Ludwig, R., and Sillmann, J.: Ten-year return levels of sub-daily extreme precipitation over Europe, *Earth Syst. Sci. Data*, 13, 983-1003, <https://doi.org/10.5194/essd-13-983-2021>, 2021.

909

910

911 Poschlod, B., Hodnebrog, Ø., Wood, R. R., Alterskjær, K., Ludwig, R., Myhre, G., and Sillmann, J.: Comparison and Evaluation of Statistical Rainfall Disaggregation and High-Resolution Dynamical Downscaling over Complex Terrain, *Journal of Hydrometeorology*, 19, 1973-1982, <https://doi.org/10.1175/jhm-d-18-0132.1>, 2018.

912

913

914 [Pui, A., Sharma, A., Mehrotra, R., Sivakumar, B., and Jeremiah, E.: A comparison of alternatives for daily to sub-daily rainfall disaggregation, *J. Hydrol.*, 470, 138– 157, <https://doi.org/10.1016/j.jhydrol.2012.08.041>, 2012.](#)

915

916

Kommentiert [ZF1]: Currently still under review.

hat formatiert: Absatz-Standardschriftart

hat formatiert: pagelast

917 Reed, C., Anderson, W., Kruczkiewicz, A., Nakamura, J., Gallo, D., Seager, R., and McDermid, S. S.: The
918 impact of flooding on food security across Africa, *Proceedings of the National Academy of*
919 *Sciences*, 119, e2119399119, <https://doi.org/10.1073/pnas.2119399119>, 2022.

920 [Sharma, A. and Srikanthan, S.: Continuous Rainfall Simulation: A Nonparametric Alternative, in:](#)
921 [30th Hydrology & Water Resources Symposium: Past, Present & Future, 4–7 December 2006,](#)
922 [Launceston, Tasmania, p. 86, 2006.](#)

923 [Stephens, A. M.: Tests based on EDF statistics. In: D'Agostino, R. B. and Stephens, M. A. \(eds.\):](#)
924 [Goodness-of-fit techniques, 1986.](#)

925 Sun, Y., Solomon, S., Dai, A., and Portmann, R. W.: How Often Does It Rain?, *Journal of Climate*, 19,
926 <https://doi.org/916-934>, 10.1175/jcli3672.1, 2006.

927 Tittensor, D. P., Novaglio, C., Harrison, C. S., Heneghan, R. F., Barrier, N., Bianchi, D., Bopp, L.,
928 Bryndum-Buchholz, A., Britten, G. L., Büchner, M., Cheung, W. W. L., Christensen, V., Coll, M.,
929 Dunne, J. P., Eddy, T. D., Everett, J. D., Fernandes-Salvador, J. A., Fulton, E. A., Galbraith, E. D.,
930 Gascuel, D., Guiet, J., John, J. G., Link, J. S., Lotze, H. K., Maury, O., Ortega-Cisneros, K., Palacios-
931 Abrantes, J., Petrik, C. M., du Pontavice, H., Rault, J., Richardson, A. J., Shannon, L., Shin, Y.-J.,
932 Steenbeek, J., Stock, C. A., and Blanchard, J. L.: Next-generation ensemble projections reveal
933 higher climate risks for marine ecosystems, *Nat Clim Change*, 11, 973-981,
934 <https://doi.org/10.1038/s41558-021-01173-9>, 2021.

935 Trinanes, J. and Martinez-Urtaza, J.: Future scenarios of risk of *Vibrio* infections in a warming planet:
936 a global mapping study, *The Lancet Planetary Health*, 5, e426-e435,
937 [https://doi.org/10.1016/S2542-5196\(21\)00169-8](https://doi.org/10.1016/S2542-5196(21)00169-8), 2021.

938 Verfaillie, D., Déqué, M., Morin, S., and Lafaysse, M.: The method ADAMONT v1.0 for statistical
939 adjustment of climate projections applicable to energy balance land surface models, *Geosci.*
940 *Model Dev.*, 10, 4257-4283, <https://doi.org/10.5194/gmd-10-4257-2017>, 2017.

941 Vormoor, K. and Skaugen, T.: Temporal Disaggregation of Daily Temperature and Precipitation Grid
942 Data for Norway, *Journal of Hydrometeorology*, 14, 989-999, [https://doi.org/10.1175/jhm-d-12-](https://doi.org/10.1175/jhm-d-12-0139.1)
943 [0139.1](https://doi.org/10.1175/jhm-d-12-0139.1), 2013.

944 Wang, K. and Clow, G. D.: The Diurnal Temperature Range in CMIP6 Models: Climatology, Variability,
945 and Evolution, *Journal of Climate*, 33, 8261-8279, <https://doi.org/10.1175/jcli-d-19-0897.1>, 2020.

946 Warszawski, L., Frieler, K., Huber, V., Piontek, F., Serdeczny, O., and Schewe, J.: The Inter-Sectoral
947 Impact Model Intercomparison Project (ISI-MIP): Project framework, *Proceedings of the National*
948 *Academy of Sciences*, 111, 3228-3232, <https://doi.org/10.1073/pnas.1312330110>, 2014.

949 [Watters, D., Battaglia, A., and Allan, R.: The Diurnal Cycle of Precipitation according to Multiple](#)
950 [Decades of Global Satellite Observations, Three CMIP6 Models, and the ECMWF Reanalysis,](#)
951 [Journal of Climate](#), 34, 5063-5080, <https://doi.org/10.1175/JCLI-D-20-0966.1>, 2021.

952 Wehner, M., Lee, J., Risser, M., Ullrich, P., Gleckler, P., and Collins, W. D.: Evaluation of extreme sub-
953 daily precipitation in high-resolution global climate model simulations, *Philosophical Transactions*
954 *of the Royal Society A: Mathematical, Physical and Engineering Sciences*, 379, 20190545,
955 <https://doi.org/10.1098/rsta.2019.0545>, 2021.

956 Zabel, F. and Mauser, W.: 2-way coupling the hydrological land surface model PROMET with the
957 regional climate model MM5, *Hydrology and Earth System Sciences*, 17, 1705–1714,
958 <https://doi.org/10.5194/hess-17-1705-2013>, 2013.

959 Zabel, F., Mauser, W., Marke, T., Pfeiffer, A., Zängl, G., and Wastl, C.: Inter-comparison of two land-
960 surface models applied at different scales and their feedbacks while coupled with a regional
961 climate model, *Hydrology and Earth System Sciences*, 16, 1017–1031,
962 <https://doi.org/10.5194/hess-16-1017-2012>, 2012.

963 Zabel, F., Müller, C., Elliott, J., Minoli, S., Jägermeyr, J., Schneider, J. M., Franke, J. A., Moyer, E., Dury,
964 M., Francois, L., Folberth, C., Liu, W., Pugh, T. A. M., Olin, S., Rabin, S. S., Mauser, W., Hank, T.,
965 Ruane, A. C., and Asseng, S.: Large potential for crop production adaptation depends on available
966 future varieties, *Global Change Biol*, 27, 3870-3882 <https://doi.org/10.1111/gcb.15649>, 2021.

967 Zhao, W., Kinouchi, T., and Nguyen, H. Q.: A framework for projecting future intensity-duration-
968 frequency (IDF) curves based on CORDEX Southeast Asia multi-model simulations: An application

hat formatiert: Absatz-Standardschriftart

969 for two cities in Southern Vietnam, *Journal of Hydrology*, 598, 126461,
970 <https://doi.org/10.1016/j.jhydrol.2021.126461>, 2021.

Seite 3: [1] hat gelöscht Zabel, Florian 01.06.23 13:35:00



Seite 3: [1] hat gelöscht Zabel, Florian 01.06.23 13:35:00



Seite 3: [1] hat gelöscht Zabel, Florian 01.06.23 13:35:00



Seite 3: [2] hat gelöscht Zabel, Florian 01.06.23 13:35:00



Seite 3: [2] hat gelöscht Zabel, Florian 01.06.23 13:35:00



Seite 3: [2] hat gelöscht Zabel, Florian 01.06.23 13:35:00



Seite 3: [2] hat gelöscht Zabel, Florian 01.06.23 13:35:00



Seite 3: [2] hat gelöscht Zabel, Florian 01.06.23 13:35:00



Seite 3: [2] hat gelöscht Zabel, Florian 01.06.23 13:35:00



Seite 3: [2] hat gelöscht Zabel, Florian 01.06.23 13:35:00



Seite 3: [3] hat formatiert Zabel, Florian 11.08.23 10:55:00

Schriftart: +Textkörper (Calibri), Schriftfarbe: Automatisch



Seite 3: [4] hat gelöscht Zabel, Florian 01.06.23 13:41:00



Seite 3: [4] hat gelöscht Zabel, Florian 01.06.23 13:41:00



Seite 3: [5] hat gelöscht Zabel, Florian 01.06.23 13:23:00



Seite 3: [5] hat gelöscht Zabel, Florian 01.06.23 13:23:00



Seite 3: [5] hat gelöscht Zabel, Florian 01.06.23 13:23:00



Seite 3: [5] hat gelöscht Zabel, Florian 01.06.23 13:23:00



Seite 3: [5] hat gelöscht Zabel, Florian 01.06.23 13:23:00



Seite 3: [5] hat gelöscht Zabel, Florian 01.06.23 13:23:00



Seite 3: [5] hat gelöscht Zabel, Florian 01.06.23 13:23:00



Seite 3: [5] hat gelöscht Zabel, Florian 01.06.23 13:23:00



Seite 3: [5] hat gelöscht Zabel, Florian 01.06.23 13:23:00



Seite 3: [5] hat gelöscht Zabel, Florian 01.06.23 13:23:00



Seite 3: [6] hat gelöscht Zabel, Florian 01.06.23 14:01:00



Seite 4: [7] hat gelöscht Zabel, Florian 07.07.23 14:10:00



Seite 4: [8] hat gelöscht Benjamin Poschlod 02.06.23 16:30:00

